Surface finishing of L-PBF Ti6Al4V ELI samples for biomedical applications by dry electro- and chemical polishing

Moses Mhlanga[1], *Lebohang R.* Masheane[1], *Ina* Yadroitsava[1], *Dean P.* Kouprianoff[1], *Gerrit M.* Ter Haar[2] and *Igor* Yadroitsev[1, 3]

[1]Department of Mechanical and Mechatronics Engineering, Central University of Technology, Bloemfontein, 9300, South Africa
[2]Department of Mechanical & Mechatronic Engineering, University of Stellenbosch, Stellenbosch 7600, South Africa
[3]Department of High-Efficiency Processing Technologies, Moscow State University of Technology "STANKIN", Vadkovskiy per. 3A, 127055, Moscow, Russia

Abstract. This study outlines a surface finishing approach for Ti6Al4V samples specifically aimed at biomedical implant applications. The process involves initial dry electropolishing (DLyte) followed by chemical polishing (CP). Three samples were fabricated using laser powder bed fusion (L-PBF) and were tested in relation to the orientation of the argon flow and powder feed direction. The effectiveness of the surface finishing process was evaluated with different combinations of polishing times. The combination of 120 minutes DLyte and 20 minutes CP achieved a surface roughness $Ra \leq 5$ µm, meeting the requirements for biocompatibility, osseointegration and implant longevity.

1 Introduction

L-PBF is a type of additive manufacturing (AM) that has attracted considerable attention in both industrial and research fields due to its ability to produce near-net-shape components with reduced production time and efficient material use. L-PBF is capable of fabricating intricate structures such as lattice structures, components with internal complexities and objects featuring functional gradients [1]. The process is conducted within a sealed build chamber filled with inert gases like nitrogen, argon, or helium. These gases are continuously circulated to maintain a protective atmosphere and prevent oxidation during fabrication. L-PBF technology has seen rapid growth across various industries, including biomedical, aerospace, and automotive and continues to expand into new areas [1]. The rough surface of objects produced by L-PBF originates from process parameters, the layer-by-layer and track-by-track nature of AM and fabrication from powder. Additionally, non-uniform gas flow within the chamber, particle size segregation and the build orientation can affect final surface roughness [1], [2]. The aforementioned factors cause the as-built Ti6Al4V L-PBF parts to typically exhibit Ra values of 5–15 µm on top surfaces and ~10–30 µm on side surfaces [3], [4]. Consequently, L-PBF parts typically exhibit higher surface roughness than what is acceptable for certain applications such as biomedical implants. In the medical field,

particularly for implants, surface quality is critical and must meet stringent surface finish standards before they can be used in the body [5], [6], [7]. For instance, dental implants require a surface roughness in the range of 1–5 µm Ra to facilitate effective osseointegration, with roughness level of approximately1–2 µm Ra promoting higher bone-to-implant contact compared to smoother surfaces [6]. Similarly, orthopedic implants such as those used in hips, knees, shoulders and the spine benefit from surface roughness between 2–5 µm Ra, which enhances bone integration and minimizes the risk of loosening [7].

To achieve the required surface roughness for biomedical implants, L-PBF-produced parts must undergo post-processing surface finishing. Several techniques are available, including manual polishing, mass finishing, burnishing, media blasting, peening, CNC machining, ultrasonic nanocrystal surface modification, electro-finishing, abrasive flow machining, electrical discharge machining (EDM), laser polishing and thermal deburring [10]. However, these methods often have limitations, especially for components with complex geometries, as they may not effectively reach all surface areas. This challenge often necessitates the use of chemical or electrochemical finishing techniques [8].

DLyte is an advanced surface finishing technique that uses a solid polymer electrolyte instead of conventional liquid-based solutions. This solid medium, infused with conductive salts, enables controlled ion exchange while reducing the environmental risks associated with hazardous liquid waste. The electrolyte composition is specifically formulated for each type of material [9]. The process integrates electrochemical dissolution, ion movement, and mechanical abrasion to selectively remove surface irregularities while preserving the part's geometry. In this setup, a metal component acts as an anode and a cathode is placed within the system. When current is applied, metal atoms oxidize and enter the electrolyte as metal ions, primarily removing surface peaks and producing a consistent polished surface [9].

Chemical polishing (CP), commonly performed with a combination of hydrofluoric acid (HF) and nitric acid (HNO_3), is widely used to smooth and brighten the surfaces of metals such as titanium, stainless steel, and aluminium [12]. This process relies on controlled chemical reactions to dissolve surface irregularities, enhancing the metal's finish. Achieving optimal results depends on carefully managing key variables like temperature, acid concentration and exposure duration [13]. HF serves as the primary etching agent, aggressively removing oxides and base metal layers, while HNO_3 acts as an oxidizer, supporting uniform material removal and reducing the risk of localized damage (such as pitting). Additionally, HNO_3 helps to passivate the metal surface [14].

2 Material and method

The specimens for this study were manufactured using the EOSINT M290 machine, employing the standard processing parameters for Ti6Al4V ELI as recommended by EOS GmbH. Three different geometries were prepared: vertical (V) with dimensions (x=5, y=20, z=20 mm), horizontal (H) with dimensions (x=20, y=20, z=5 mm) and semispherical (S) samples with a 20 mm diameter. All samples were produced from gas atomised Ti6Al4V ELI powder comprising of spherical particles with a size range of 15–75 µm. These specimens were categorized into zones 1 to 9 based on the argon gas flow direction (inlet and outlet) and the starting and ending positions of the powder bed, as illustrated in **Fig. 1**. Additionally, extra semi-spherical samples were manufactured with a holder (see **Fig. 2**c) designed to fit the clamps of the dry electropolishing system. The holder measurements were (x=2, y=4, z=4 mm). These additional samples were produced under the same conditions as the others in **Fig. 1**.

Post-processing involved stress relieving at 650°C for 3h followed by annealing at 950°C for 2h in a vacuum furnace as described by Yadroitsev *et al* [15]. The vertical samples (**Fig. 2**a) were designated for studying surface finishing along the sides (inter-layer surfaces), while

the horizontal samples (**Fig. 2**b) were designed to study the top surface roughness. The semi-spherical samples (**Fig. 2**c) were created to assess surface finishing on L-PBF parts with a pronounced stair-step effect. Scanning Electron Microscopy (SEM) images were captured after dry electropolishing and chemical polishing using a NeoScope 3000 at various magnifications at a voltage of 20KV working distance between 30 mm to 41 mm and SEM mode: secondary electron.

Mass measurements before and after chemical polishing were performed with an ABT 120-5DNM analytical balance with a readability (resolution): 0.01 mg (0.00001 g), and the solution temperature was recorded after each chemical polishing duration using a Fluke 568EX infrared thermometer. Prior to imaging and polishing, the samples were cleaned in an ultrasonic bath using acetone, ethanol, and distilled water sequentially. Each cleaning step lasted between 15 and 30 minutes following standard protocols for biomedical implants [16].

The effectiveness of the surface finishing process using dry electropolishing followed by chemical polishing was evaluated based on treatment duration. Three different time combinations were examined: 30 minutes DLyte followed by 5 minutes CP, 60 minutes DLyte followed by 10 minutes CP and 120 minutes DLyte followed by 20 minutes CP. The dry electropolishing was carried out using a DLyte 100H machine, applying the standard process parameters and the Ti Group - Ti01 electrolyte specifically designed for Ti6Al4V [11].

Post DLyte of the samples was CP using a mixture of HF and HNO_3 as outlined in [17]. A single solution composition was used with the initial nitric acid concentration fixed at 3.17 M (Molarity) and a weight ratio of HF to HNO_3 of 1:2.5. The etching solution 650 mL was prepared in 1000 mL high-density polyethylene (HDPE) containers, which were subsequently placed in an ice bath housed within a secondary polypropylene (PP) container as illustrated in **Fig. 3** . The solution was magnetically stirred at 400 rpm to ensure uniform etching across the sample surfaces. Three samples per composition were processed simultaneously in each container. For safe handling, the samples were suspended using HDPE strings secured to the container lids. No additional acid was introduced during the polishing process, nor was the solution volume intentionally altered. The temperature of the etchant was recorded after each polishing interval. The effectiveness of CP after DLyte treatment was assessed with three different polishing times: 5, 10, and 20 minutes.

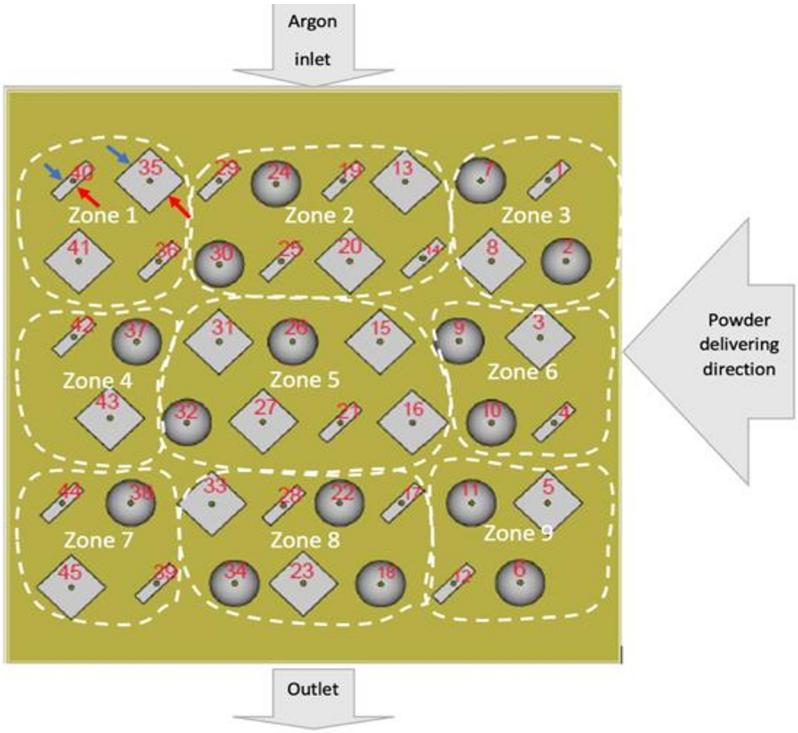

Fig. 1. View of the substrate showing the positions of samples and their zones.

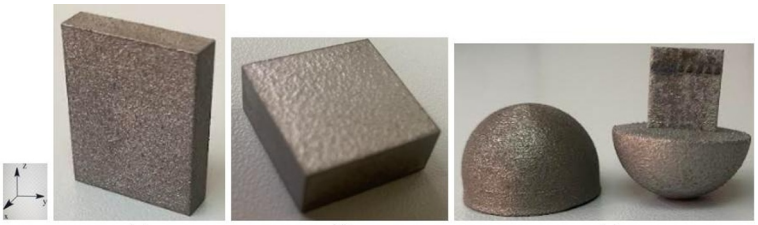

Fig. 2. Photographs of: (a) **v**ertical, (b) horizontal, and (c) semi-sphere and semi-sphere with a holder Ti6Al4V manufactured and heat-treated samples.

Three distinct regions were identified for analysis: Zone 3, located near both the argon gas inlet and the starting point of the powder recoater; Zone 5, situated at the center of the build plate; and Zone 7, positioned furthest from both the argon inlet and recoater starting area, **Fig. 1**. Vertical samples were selected from each zone sample 1 from Zone 3, sample 21 from Zone 5, and sample 44 from Zone 7. The vertical samples were sectioned along the orange dotted lines shown in **Fig. 4**a. One segment from each was kept in the as-built state, while the other three segments underwent surface finishing using DLyte followed by CP.

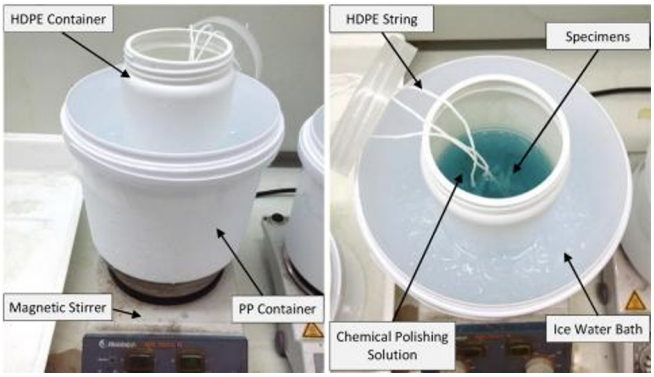

Fig. 3. Photograph of the chemical polishing set-up [17].

Similarly, horizontal samples from the same zones were chosen: sample 8 from Zone 3, sample 27 from Zone 5, and sample 45 from Zone 7. Each horizontal sample was divided into four segments, indicated by the orange dotted line in **Fig. 4**b. One segment was analyzed in the as-built state and the remaining three underwent the same surface finishing treatment. Additionally, semispherical samples designated for surface finishing were from Zone 3 samples 1a, 2a, and 3a; Zone 5 samples 4a, 5a, and 6a; and Zone 7 samples 7a, 8a, and 9a. These samples were previously studied in the as-built condition in [18] and with DLyte only [15]. The current surface treatments, including both dry electropolishing and subsequent chemical polishing, were performed in accordance with **Table 1**.

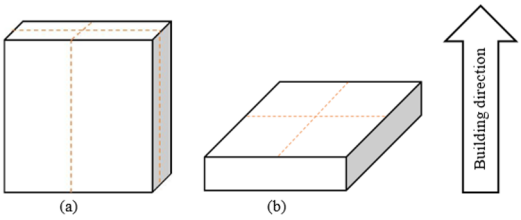

Fig. 4. Vertical (a) and horizontal (b) segmented samples.

Table 1. Selected samples for polishing.

DLyte followed by chemical polishing in HF-HNO3 solutions				
Zones	**Semi-sphere**	**Vertical**	**Horizontal**	**Polishing duration**
Zone 3	#1a, #2a, #3a	sample #1	sample #8	30 min Dlyte + 5 min CP 60 min Dlyte + 10 min CP 120 min Dlyte + 20 min CP
Zone 5	#4a ,#5a, #6a	sample #21	sample #27	
Zone 7	#7a, #8a, #9a	sample #44	sample #45	

Surface roughness parameters including average roughness (Ra), root mean square roughness (Rq), and ten-point height (Rz), were evaluated after DLyte and CP using a Mitutoyo Surftest SJ-210 profilometer. Measurements were taken at three randomly chosen locations on each sample. For horizontal samples, the roughness was measured along the inter-track on the top surface, while for vertical samples it was assessed on the side surface in a direction perpendicular to the build, i.e., along the build direction. Each vertical and horizontal sample was measured using a cut-off length of 0.8 mm and an evaluation length

of 4 mm. In contrast, semi-spherical samples required a different setup; a custom jig/fix [15] was used to assess their surface roughness using the Mitutoyo Surftest SJ-210, following ISO 427:1997, with a cut-off length of 2.5 µm and an evaluation length of 0.25 mm for each measurement.

3 Results and discussion

3.1 Results of 30 minutes dry electropolishing and followed by 5 minutes chemical polishing

Fig. 5-Fig. 7 illustrates the surface roughness measurements of the vertical (V) (side surface), horizontal (H) (top surface), and semispherical (S) surfaces after 30 minutes DLyte followed by an additional 5 minutes CP. In all the zones, the surface roughness further decreased after the CP. The most significant reduction in Ra after this process was recorded in Zone 3, for the semisphere samples, with a Ra of 5.1 µm, while Zone 7 exhibited the least reduction. Additionally, both the top and side surfaces also displayed a decreased surface roughness for all zones after 5 minutes CP. The trends of Rq and Rz were similar to Ra, with the greatest reductions occurring in Zone 3 and the least in Zone 7. After 5 minutes CP, the solution's temperature was measured at 20 °C, and the weight loss was relatively minor compared to the losses observed at 10 and 20 minutes CP.

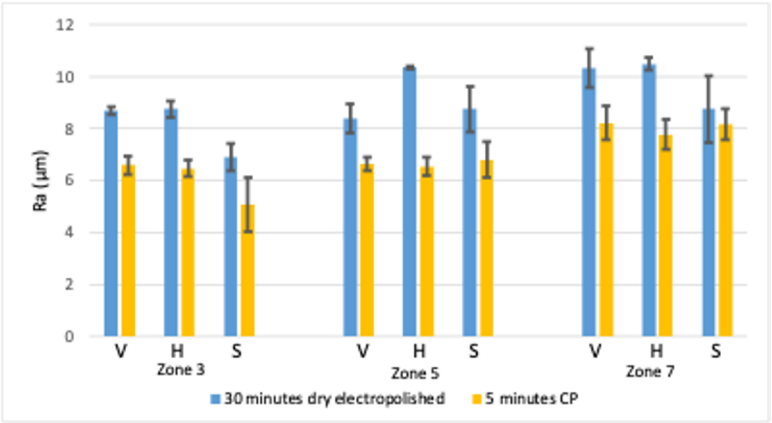

Fig. 5. Ra 30 minutes Dlyte followed by 5 minutes CP.

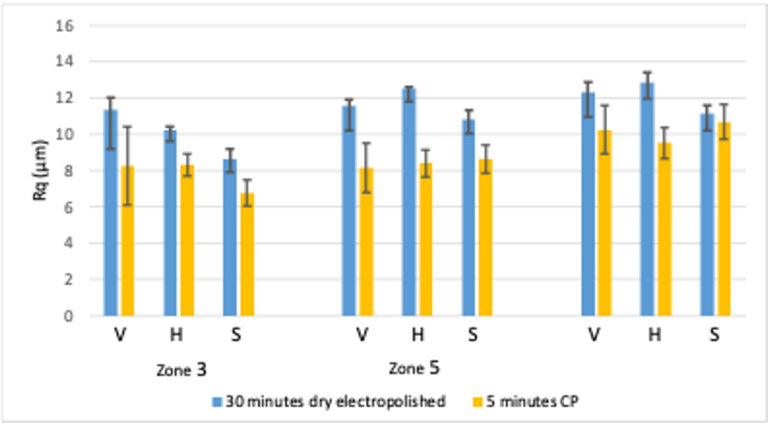

Fig. 6. Rq 30 minutes DLyte followed by 5 minutes CP.

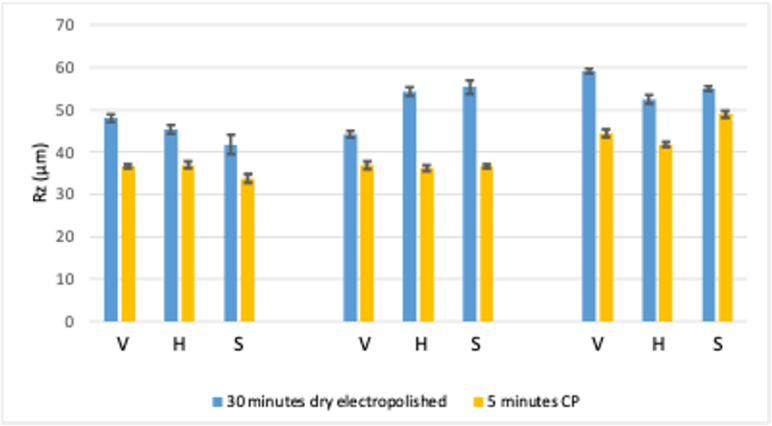

Fig. 7. *Rz* 30 minutes DLyte followed by 5 minutes CP.

Fig. 8 presents the SEM images of surface finishing after 30 minutes DLyte followed by 5 minutes CP. A notable decrease in the presence of attached powder particles is evident across all samples in every zone compared to the results of the 30 minutes DLyte. Vertical samples exhibited melted-like attached powder particles in all zones after 5 minutes CP. The horizontal samples retained some visibility of tracks, peaks and valleys along with a reduced number of attached powder particles after the 5 minutes CP. In the semisphere samples, there was an evident removal of attached powder particles and contour marks across all zones; however, the stair-step patterns remained visible in all samples.

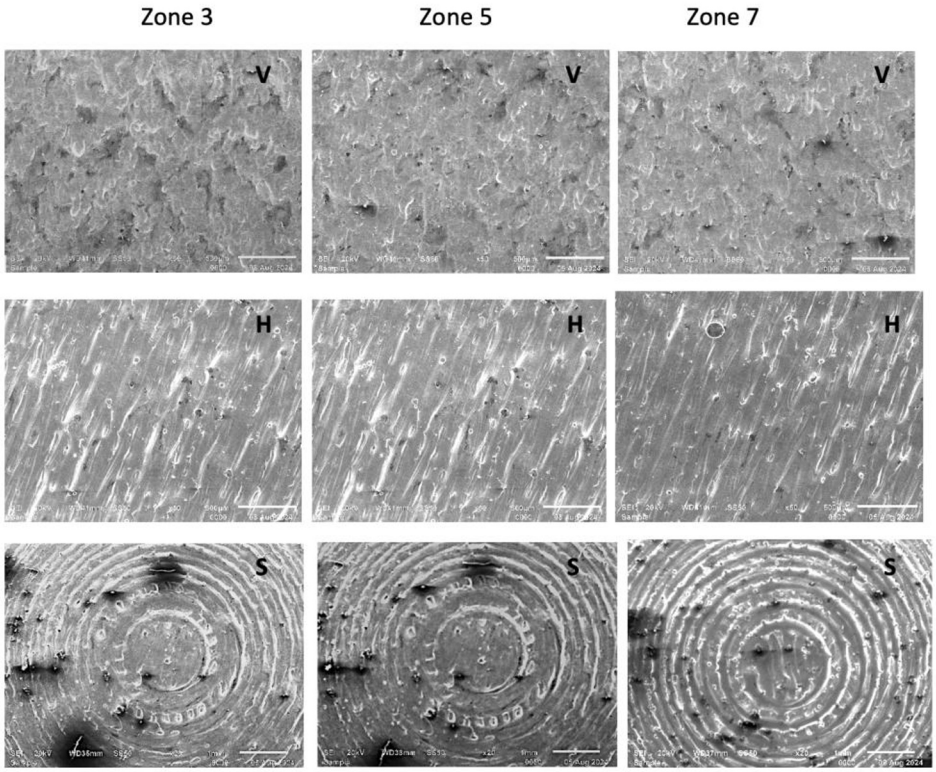

Fig. 8. SEM images of 30 minutes DLyte followed by 5 minutes CP.

3.2 Results of 60 minutes of dry electropolishing followed by 10 minutes of chemical polishing

Fig. 9-Fig. 11 illustrate the outcomes for Ra, Rq, and Rz after a 60 DLyte process followed by 10 minutes CP. A reduction in the surface roughness parameters is evident. The vertical, horizontal and semispherical surfaces display additional decreases in Ra, Rq and Rz after CP phase. It is noted that the duration of CP is directly proportional to the reduction observed in Ra, Rq and Rz. Prolonging the duration of CP leads to a rise in the chemical solution temperature. After 5 minutes of CP, the temperature reaches 20 °C, while it increases to 25 °C after 10 minutes of CP. This escalation can lead to accelerated material removal, localized overheating, pitting, or surface roughening of the titanium alloy, ultimately resulting in a loss of mass.

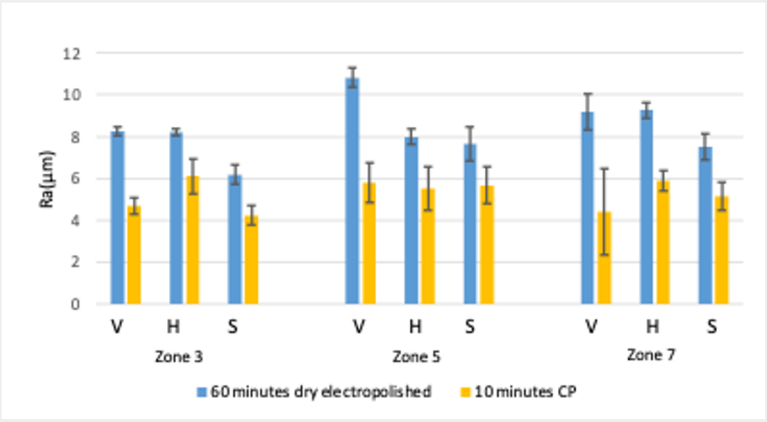

Fig. 9. *Ra* after 60 minutes DLyte followed by 10 minutes CP.

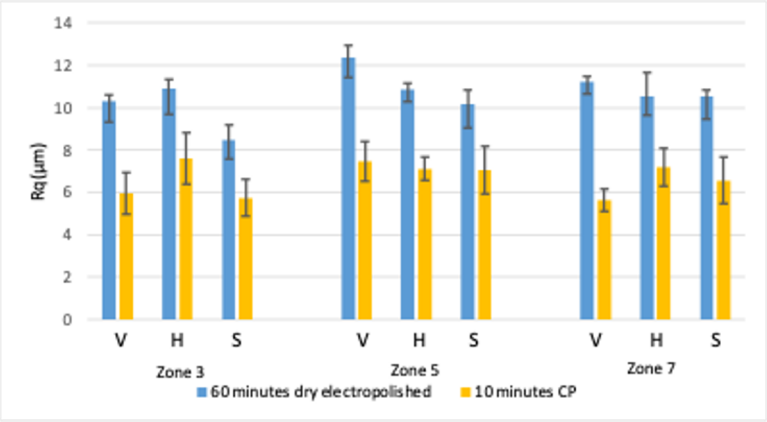

Fig. 10. *Rq* after 60 minutes DLyte followed by 10 minutes CP.

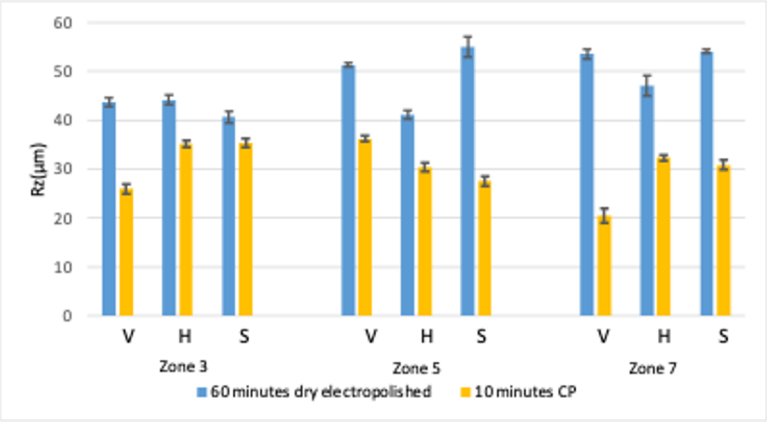

Fig. 11. *Rz* after 60 minutes DLyte followed by 10 minutes CP.

Fig. 12 shows the SEM images of vertical, horizontal and semispherical samples that were polished for 60 minutes DLyte followed by 10 minutes CP. There was notable removal of powder particles attached to the surface of the vertical samples until a smooth surface emerges in all zones. However, the smooth surfaces were not uniform, as peaks and valleys are visible on the surface of the vertical samples in all the zones. There was continual removal of attached powder particles, resulting in a smooth horizontal surface. The peaks and valleys due to tracks during the building were still visible. The observed reduction in contour, the presence of attached powder particles, and the formation of staircases were noted in the semisphere sample.

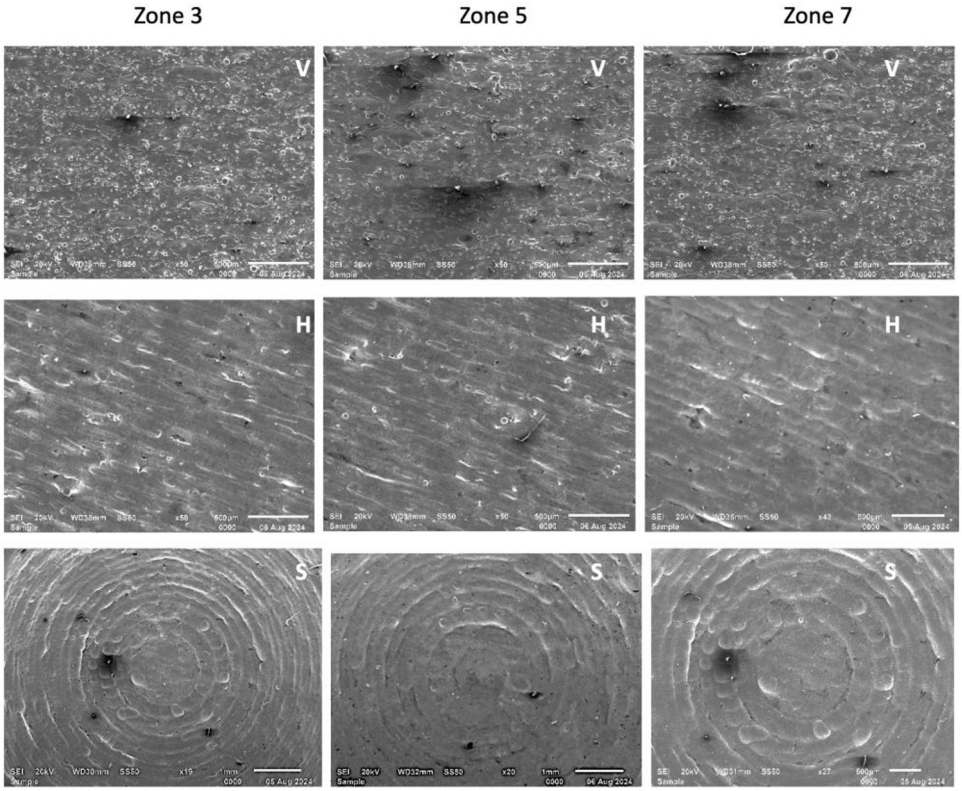

Fig. 12. SEM images of 60 minutes DLyte followed by 10 minutes CP.

3.3 120 minutes of dry electropolishing followed by 20 minutes of chemical polishing

The most significant reductions in Ra, Rq, and Rz were recorded after 120 minutes of DLyte, with this effect being further enhanced by an additional 20 minutes of CP, particularly in contrast to the 5 minutes and 10 minutes of CP, as demonstrated in **Fig. 13Fig. 15**. Following a 20 minutes' period of CP, Zone 3 recorded the lowest roughness, whereas Zone 7 exhibited the highest roughness level. The rise in CP duration correlated with a significant reduction in Ra values. The minimum Ra observed was 2.858 µm in Zone 3, while the maximum after chemical polishing reached 3.875 µm in Zone 7. Rq and Rz displayed a similar pattern to Ra. After 20 minutes CP, the solution's temperature reached 40 °C due to the extended polishing duration. Across all surfaces, including the sides, top and semisphere, there was a significant reduction in surface roughness after 20 minutes of chemical polishing.

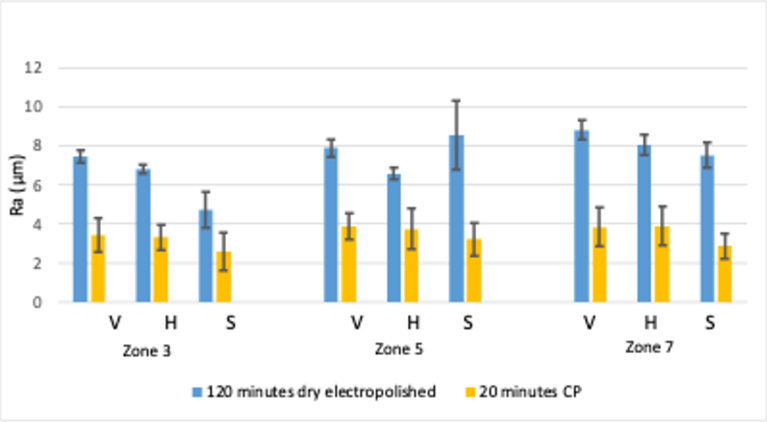

Fig. 13. *Ra* after 120 minutes DLyte followed by 20 minutes CP.

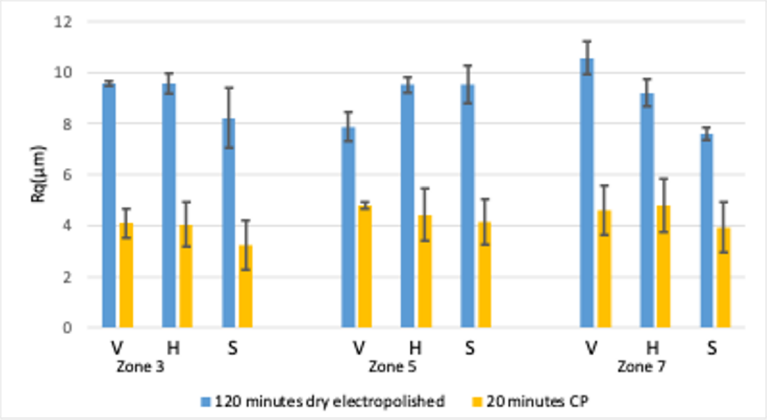

Fig. 14. *Rq* after 120 minutes DLyte followed by 20 minutes CP.

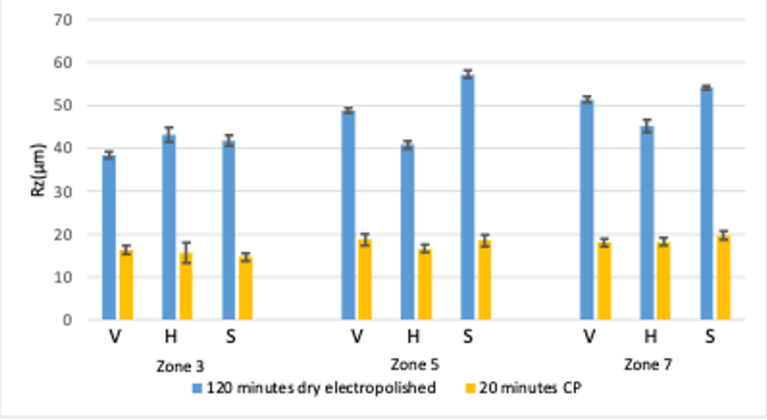

Fig. 15. *Rz* of 120 minutes Dlyte followed by 20 minutes CP.

Fig. 16 shows the SEM images of the vertical, horizontal and semisphere samples that were polished for 120 minutes Dlyte followed by 20 minutes CP. After polishing, nearly all attached powder particles, peaks and valleys were removed, resulting in a smooth surface on the vertical samples across all zones. The peaks and valleys due to tracks were still noticeable in the horizontal samples. Nearly all the attached powder particles, contours, and staircases on the surface of the semisphere were removed; however, the surface was not uniform. Chemical polishing improves overall smoothness but introduces dimpling or localized roughness.

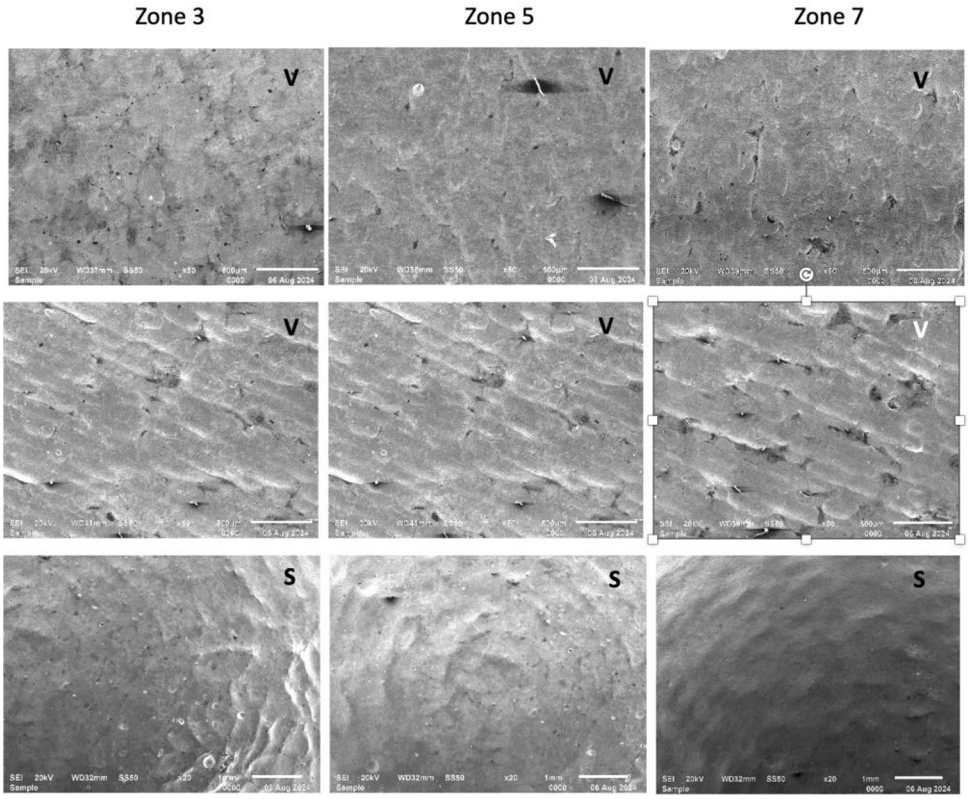

Fig. 16. SEM images of 120 minutes DLyte followed by 20 minutes CP.

3.4 Weight loss before and after chemical polishing

After CP, the surface quality of the samples across all zones showed considerable enhancement. Nevertheless, it was observed that as the surface roughness improved, there was a corresponding increase in the mass loss of the components. A trend was noted where the mass of the components diminished as the duration of CP was extended. **Fig. 17**-**Fig. 19** depict the mass of the components before and after 5, 10, and 20 minutes CP. Across all zones and forms, vertical, horizontal, and semisphere mass loss was evident throughout all durations of CP. This phenomenon is attributed to the extended polishing time.

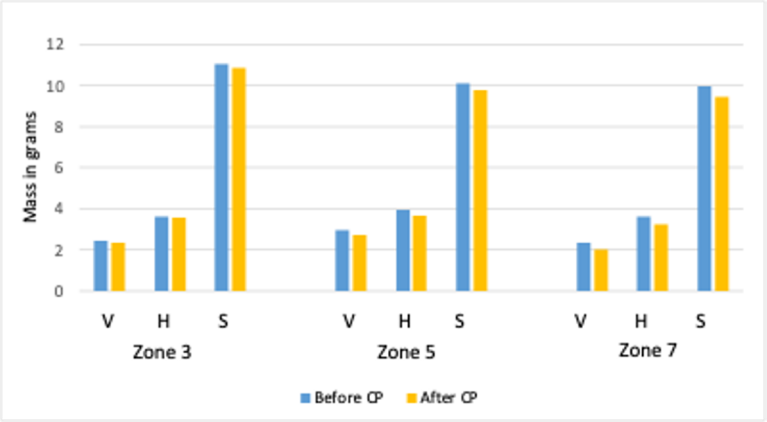

Fig. 17. Mass loss after 5 minutes CP.

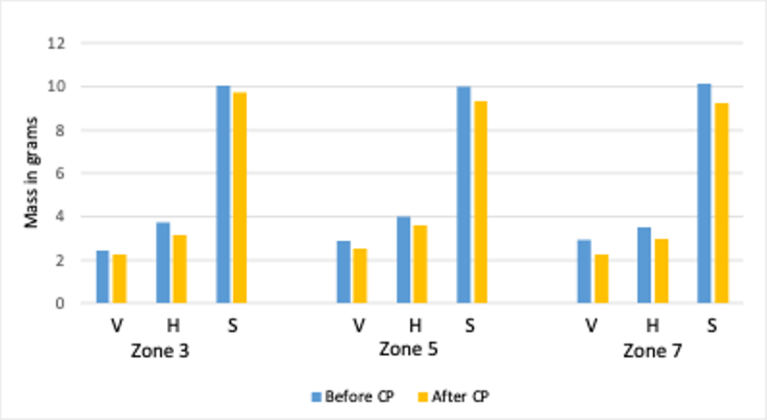

Fig. 18. Mass loss after 10 minutes CP.

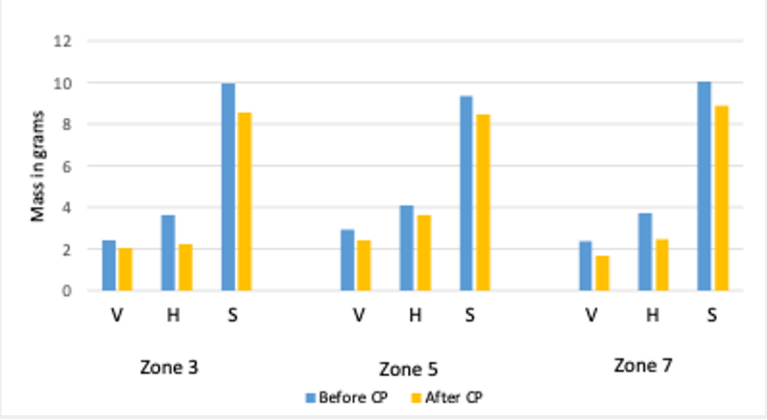

Fig. 19. Mass loss after 20 minutes CP.

The longer the CP duration, the better the achieved surface roughness, although there is an increase in mass loss during the process in HF and HNO3 solutions. The loss of mass is due to higher temperatures that speed up chemical reactions, leading to an accelerated material removal, localized overheating, pitting, or surface roughening of the titanium alloy as stated in [19].

4 Conclusions

- The combination of DLyte and CP in HF and HNO_3 solution shows the surface roughness of $Ra \leq 5$ µm required for biocompatibility, osseointegration and longevity in medical implants after 120 minutes DLyte followed by 20 minutes CP.
- After 30 and 60 minutes, Dlyte followed by 5 and 10 minutes CP, respectively, there is a fluctuation of Ra, mostly $Ra > 5$µm.
- As the CP duration increased, mass loss also increased.
- After 20 minutes DLyte followed by 20 minutes CP, $Ra \leq 5$µm is achieved; however, this comes at the expense of mass loss.
- After 30 and 60 minutes DLyte followed by 5 and 10 minutes CP, the results show Ra>5 µm. However, the mass loss is lower compared to 120 minutes Dlyte followed by 20 minutes CP.
- The loss of mass is due to extending the time for CP that leads to an increase in the chemical solution temperature, which can cause accelerated material removal, localized overheating, pitting, or surface roughening of the titanium alloy

A special word of appreciation to the South African Research Chairs Initiative of the Department of Science and Innovation and the National Research Foundation of South Africa (Grant № 97994) and the Collaborative Program in Additive Manufacturing (Contract № CSIR-NLC-CPAM-21-MOA-CUT-03) for the financial aid received for financial support and CRPM for manufacturing parts.

References

[1] I. Yadroitsev, I. Yadroitsava, A. Du Plessis and E. Macdonald, Fundamentals of Laser Powder Bed Fusion of Metals, March, (2021). https://doi.org/10.1016/C2020-0-01200-4

[2] J. C. Snyder and K. A. Thole, Understanding laser powder bed fusion surface roughness, ASME, **142**, 7 (2020). https://doi.org/10.1115/1.4046504

[3] W. M. I. Makhetha, T. H. Becker, and N. Sacks, Post-Processing Framework for As-Built LPBF Ti-6Al-4V Parts Towards Meeting Industry Functional Requirements, **74**, 764–776 (2022), https://doi.org/10.1007/s11837-021-05078-y

[4] A. Yánez, M. P. Fiorucci, O. Martel, and A. Cuadrado, The Influence of Dimensions and Powder Recycling on the Roughness and Mechanical Properties of Ti-6Al-4V Parts Fabricated by Laser Powder Bed Fusion, **15**, 16 (2022). https://doi.org/10.3390/ma15165787

[5] P. Thomsen, Material Science, Surface Science, Engineering , Biological Responses, (2001).

[6] A. G. Harvey, E. W. Hill, and A. Bayat, Designing implant surface topography for improved biocompatibility, **10**, 2, pp. 257–267, (2013). https://doi.org/10.1586/erd.12.82

[7] T. Albrektsson and A. Wennerberg, On osseointegration in relation to implant surfaces, **21**, pp. 4–7 (2019). https://doi.org/10.1111/cid.12742.

[8] D. Buser *et al.*, Long-term stability of early implant placement with contour augmentation, **92**, no. 12, (2013). https://doi.org/10.1177/0022034513504949.

[9] A. Jemat, M. J. Ghazali, M. Razali, and Y. Otsuka, "Surface modifications and their effects on titanium dental implants, (2015). https://doi.org/10.1155/2015/791725.

[10] P. S. Sibanda, P. Carr, M. Ryan, and S. Bigot, State of he Art in Surface Finish of Metal Additive Manufactured Parts, **9**, November, pp. 221–225, (2019).

[11] Surface Finishing using Dry Electro-polishing Machines Comparison Surface Finishing Process for Machining Implants. https://metrotool.co.za/wp-content/uploads/2022/04/Surface-Finishing-using-Dry-Electro-polishing-Machines.pdf

[12] A. Chmielewska, A. Jahadakbar, B. Wysocki, M. Elahinia, W. Święszkowski, and D. Dean, Chemical Polishing of Additively Manufactured, Porous, Nickel-Titanium Skeletal Fixation Plates, **9**, 4, pp. 269–277, (2022). https://doi.org/10.1089/3dp.2020.0209

[13] P. Lanfermann, C. Weidmann, M. C. Maaß, S. Waitz, T. Schönberger, and T. Waitz, Electrochemical surface modification of titanium in Chemistry Class, **11**, pp. 2–6, (2022).

[14] M. A. Obeidi, Results in Engineering Metal additive manufacturing by laser-powder bed fusion : Guidelines for process optimisation, **15**, May,100473 (2022). https://doi.org/10.1016/j.rineng.2022.100473

[15] I. Yadroitsev, P. Krakhmalev, and I. Yadroitsava, Selective laser melting of Ti6Al4V alloy for biomedical applications: Temperature monitoring and microstructural evolution, **583**, 404–409 (2014). https://doi.org/10.1016/j.jallcom.2013.08.183

[16] Cleaning and sterilization Guidelines for Nobel Biocare products including MRI information, *Nobel Biocare*.

[17] M. Bezuidenhout, G. Ter Haar, T. Becker, S. Rudolph, O. Damm, and N. Sacks, The effect of HF-HNO3 chemical polishing on the surface roughness and fatigue life of laser powder bed fusion produced Ti6Al4V, **25**, June,101396, (2020). https://doi.org/10.1016/j.mtcomm.2020.101396

[18] M. Mhlanga, L. R. Masheane, I. Yadroitsava, and I. Yadroitsev, Surface roughness of Ti6Al4V samples produced by laser powder bed fusion for bone implants, **370**, 11001, (2022). https://doi.org/10.1051/matecconf/202237011001

[19] Y. Wang, H. Liu, X. Yin, Y. Zhou, M. Feng, and S. Li, Study on electrochemical polishing mechanism of TC4 titanium alloy ,**99**, 85983 (2024). https://doi.org/10.1088/1402-4896/ad63e1.